Specifications and Pre-production of n^{+}-in-p Large-format Strip Sensors fabricated in 6-inch Silicon Wafers, ATLAS18, for the Inner Tracker of the ATLAS Detector for High-Luminosity Large Hadron Collider

Y. Unno[f,1] **H. Abidi**[k] **A. Affolder**[i] **K. Affolder**[i] **P.P. Allport**[a] **S. Beaupre**[j,l] **G.A. Beck**[h] **J. Bernabeu**[e] **A.J. Bevan**[h] **A. Chisholm**[a] **B. Ciungu**[k] **I. Dawson**[h] **A. Dowling**[i] **V. Fadeyev**[i] **P. Federicova**[g] **J. Fernandez-Tejero**[j,l] **C. Fleta**[d] **A. Fournier**[j,l] **W. George**[a] **M. Gignac**[i] **L. Gonella**[a] **G. Greig**[j,l] **J. Gunnell**[i] **K. Hara**[m] **S. Hirose**[m] **B. Hommels**[b] **T. Ishii**[m] **C. Jessiman**[c] **J. Johnson**[i] **D. Jones**[b] **S. Kachiguin**[i] **N. Kang**[i] **J. Keller**[c] **C. Klein**[c] **T. Koffas**[c] **I. Kopsalis**[a] **J. Kroll**[g] **J. Kvasnicka**[g] **C. Lacasta**[e] **V. Latonova**[g] **J. Lomas**[a] **F. Martinez-Mckinney**[i] **M. Mikestikova**[g] **P.S. Miyagawa**[h] **R.S. Orr**[k] **L. Poley**[j,l] **D. Rousso**[b] **A. Shah**[h] **C. Solaz**[e] **U. Soldevila**[e] **E. Staats**[c] **T.L. Stack**[j,l] **B. Stelzer**[j,l] **M. Ullan**[d] **J. Yarwick**[i] **S.C. Zenz**[h]

[a] *School of Physics and Astronomy, University of Birmingham, Birmingham B152TT, United Kingdom*
[b] *Cavendish Laboratory, University of Cambridge, JJ Thomson Avenue, Cambridge CB3 0HE, United Kingdom*
[c] *Physics Department, Carleton University, 1125 Colonel By Drive, Ottawa, Ontario, K1S 5B6, Canada*
[d] *Instituto de Microelectronica de Barcelona (IMB-CNM, CSIC), Campus UAB-Bellaterra, 08193 Barcelona, Spain*
[e] *Instituto de Física Corpuscular, IFIC/CSIC-UV, C/Catedrático José Beltrán 2, E-46980 Paterna, Valencia, Spain*
[f] *Institute of Particle and Nuclear Study, High Energy Accelerator Research Organization (KEK), 1-1 Oho, Tsukuba, Ibaraki 305-0801, Japan*
[g] *Institute of Physics, Academy of Sciences of the Czech Republic, Na Slovance 2, 18221 Prague 8, Czech Republic*
[h] *Department of Physics and Astronomy, Queen Mary University of London, London, E1 4NS, United Kingdom*
[i] *Santa Cruz Institute for Particle Physics (SCIPP), University of California, Santa Cruz, CA 95064, USA*
[j] *Department of Physics, Simon Fraser University, 8888 University Drive, Burnaby, B.C. V5A 1S6, Canada*
[k] *Department of Physics, University of Toronto, 60 Saint George St., Toronto, Ontario M5S1A7, Canada*
[l] *TRIUMF, 4004 Wesbrook Mall, Vancouver, B.C. V6T 2A3, Canada*
[m] *Institute of Pure and Applied Sciences, University of Tsukuba, 1-1-1 Tennodai, Tsukuba, Ibaraki 305-8571, Japan*

E-mail: yoshinobu.unno@kek.jp

ATL-ITK-PROC-2022-016
13/03/2023

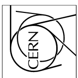

[1] Corresponding author.

Abstract: The ATLAS experiment is constructing new all-silicon inner tracking system for HL-LHC. The strip detectors cover the radial extent of 40 to 100 cm. A new approach is adopted to use p-type silicon material, making the readout in n^+-strips, so-called n^+-in-p sensors. This allows for enhanced radiation tolerance against an order of magnitude higher particle fluence compared to the LHC. To cope with varying hit rates and occupancies as a function of radial distance, there are two barrel sensor types, the short strips (SS) for the inner 2 and the long strips (LS) for the outer 2 barrel cylinders, respectively. The barrel sensors exhibit a square, $9.8 \times 9.8\,\mathrm{cm}^2$, geometry, the largest possible sensor area from a 6-inch wafer. The strips are laid out in parallel with a strip pitch of 75.5 µm and 4 or 2 rows of strip segments. The strips are AC-coupled and biased via polysilicon resistors. The endcap sensors employ a "stereo-annulus" geometry exhibiting a skewed-trapezoid shapes with circular edges. They are designed in 6 unique shapes, R0 to R5, corresponding to progressively increasing radial extents and which allows them to fit within the petal geometry and the 6-inch wafer maximally. The strips are in fan-out geometry with an in-built rotation angle, with a mean pitch of approximately 75 µm and 4 or 2 rows of strip segments. The eight sensor types are labeled as ATLAS18xx where xx stands for SS, LS, and R0 to R5. According to the mechanical and electrical specifications, CAD files for wafer processing were laid out, following the successful designs of prototype barrel and endcap sensors, together with a number of optimizations. A pre-production was carried out prior to the full production of the wafers. The quality of the sensors is reviewed and judged excellent through the test results carried out by vendor. These sensors are used for establishing acceptance procedures and to evaluate their performance in the ATLAS collaboration, and subsequently for pre-production of strip modules and stave and petal structures.

Keywords: Si microstrip and pad detectors, Radiation-hard detectors, Particle tracking detectors (Solid-state detectors)

Contents

1 Introduction **1**

2 ATLAS silicon strip sensor for HL-LHC **3**
- 2.1 Barrel sensors: ATLAS18SS and ATLAS18LS 4
- 2.2 Endcap sensors: ATLAS18R0, ATLAS18R1, ATLAS18R2, ATLAS18R3, ATLAS18R4, ATLAS18R5 7
- 2.3 Fiducial markers of endcap sensors 9

3 Wafer layouts **11**
- 3.1 Wafer layouts of ATLAS18 sensors 11
- 3.2 Miniature sensors and test structures 12

4 Electrical Properties **16**
- 4.1 Electrical properties common to all types of sensors 16
- 4.2 Tests carried out by vendor 16

5 Pre-production of ATLAS18 sensors/wafers **17**

6 Conclusion **25**

A Formulation of the strips of the endcap sensors **25**

B ATLAS Upgrade serial number **25**

C Identification pad and scratch pads **26**

1 Introduction

ATLAS is constructing an all-silicon inner tracking system[1] for the high-luminosity large hadron collider (HL-LHC), to cope with a peak instantaneous luminosity of $\mathscr{L}$ =7.5×10^{34} cm^{-2}s^{-1} with 200 simultaneous events per beam crossing, and an integrated luminosity of 4000 fb^{-1} [1]. The tracking system will be made of silicon pixel detectors in the inner part and silicon strip detectors in the outer part, and reside inside a 2 Tesla ATLAS solenoid magnet. The strip detectors are in the radial extent of 40 to 100 cm, made of four concentric cylinders in the central region (barrel) and six disks on each side of endcap regions. A cylinder in the barrel or a disk in the endcap is composed of a structure called “stave” or “petal”, respectively. A stave is made of 14 modules per side, with a common nearly-square single-sided sensor for each module. The modules are rotated

[1]These instantaneous and integrated luminosities are approximately five and ten times of the end-of-life goals of LHC, respectively

by 26 milli-radian (mrad) to the stave axis for stereo hit reconstruction[2] (Fig. 1a). A petal is made of 9 modules per side, with unique shapes of sensors in each radial extent from $R0$ to $R5$ (Fig. 1b), with a rotation angle of 20 mrad to the radial axis of the sensor built in the strips[3]. An expanded view of endcap sensor (R0) is shown in Fig. 1c with the legends being defined in Sections 2.2 and 2.3.

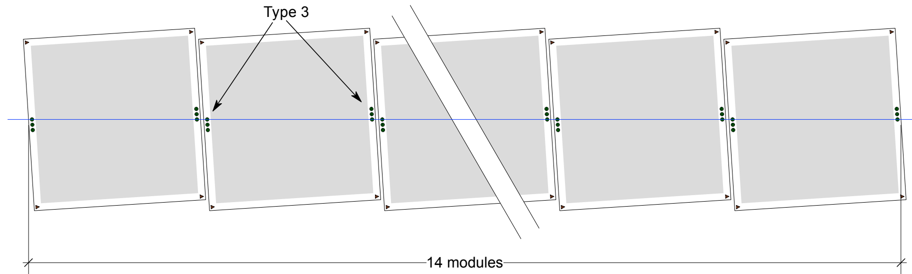

(a) A "Stave" with 14 barrel modules on either the front or back side in the barrel cylinder. Modules are rotated by 26 mrad to the stave axis. Those triplet of fiducial markers,Type 3, are the stereo fiducial markers (cf. Fig. 2a).

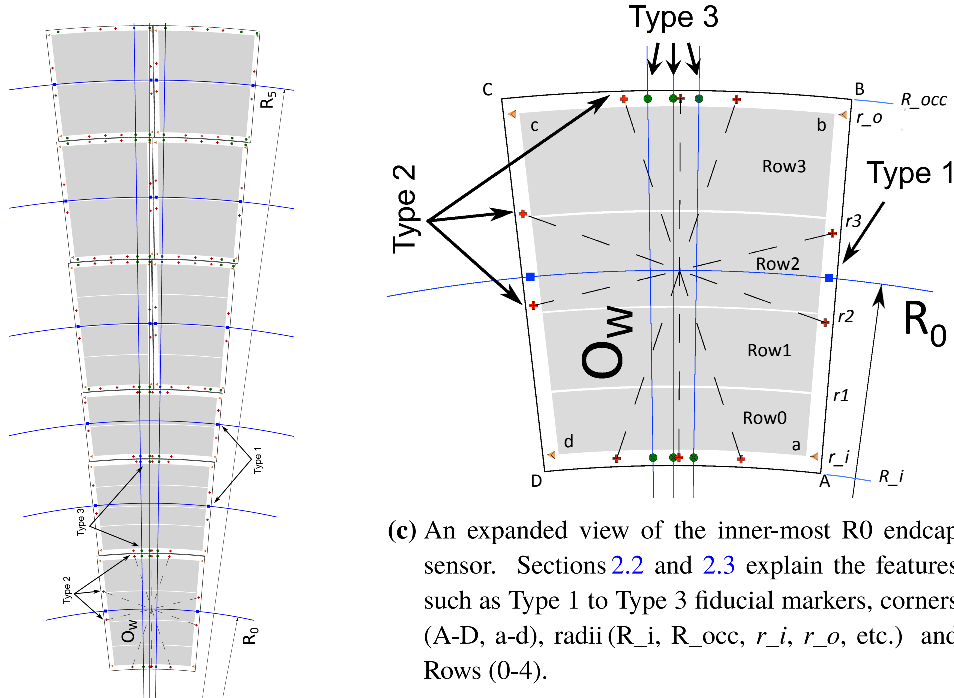

(b) A "Petal" with 9 endcap modules per Petal side in the endcap disks. The rotation angle of 20 mrad to the radial axis of the sensor is built in the strips.

(c) An expanded view of the inner-most R0 endcap sensor. Sections 2.2 and 2.3 explain the features such as Type 1 to Type 3 fiducial markers, corners (A-D, a-d), radii (R_i, R_occ, *r_i*, *r_o*, etc.) and Rows (0-4).

Fig. 1: Schematic views of (a) Stave, (b) Petal, and (c) R0 sensor.

[2]It is 3D hit reconstruction together with the radial coordinate of the stave. The stereo angle made by the front and the "180° flipped" back sides is twice the rotation angle. The total number of modules, per "stave" or "petal", is twice the number of modules per side.

[3]The sensors are not rotated in the petal, unlike the stave case.

The sensors are in the same plane, separated by a gap of 500 µm from their neighbors. With a cylinder or a disk being made of a layer of single-sided strip sensors on both the front and the back sides of the structure, the strip system is composed of 10976 barrel and 6912 endcap sensors, with a total area of 165 m^2[1].

2 ATLAS silicon strip sensor for HL-LHC

The maximum fluence and the maximum ionizing dose of the innermost part of the barrel are anticipated to be approximately 9.7×10^{14} n_{eq}/cm^2 and 44 Mrad, and 1.6×10^{15} n_{eq}/cm^2 and 66 Mrad, respectively for the endcap, including a safety factor of 1.5. Under intense irradiation, silicon sensors change their device properties significantly. The damage in the bulk modifies the sensor's depletion characteristics. With defect levels of p-type being created dominantly, the full depletion voltage has risen to over one thousand volts for a typical 300 µm thick silicon sensor. The damage in the surface raises the oxide-silicon interface charge by an order of magnitude. The design goals of the radiation-tolerant strip sensor are to achieve high voltage operation by avoiding high field regions and possible breakdowns and high strip isolation with low strip capacitance.

The strip sensor for the current ATLAS semiconductor tracker (SCT) for LHC [2] is made with p^+-strips in an n-bulk silicon wafer, so-called p^+-in-n sensor. The p^+-in-n sensor requires nearly full depletion after a fluence of a few times 10^{13} n_{eq}/cm^2 of particles. This is because the n-type material converts to a p-type under irradiation and the depletion region originates from the backside. We have chosen a new approach for HL-LHC to use non-inverting p-type material with the readout in n^+-strips, so-called n^+-in-p sensor, ensuring the origination of the depletion region from the strip side at any fluence. The n^+-in-p sensor enables the sensor operation in partially depleted mode above a fluence where the full depletion of the bulk is no longer achievable. It allows single-side wafer processing, making the sensor more affordable than the n^+-in-n sensor, another type of sensor with n^+-strip readout but which requires double-side wafer processing. We have developed and optimized the design in 6-inch (150 mm wafer diameter) wafer process[4] through prototype sensors of ATLAS07[3], ATLAS12[4], ATLAS12EC/R0[5], and ATLAS17LS[6], to the ATLAS18 for the production sensors.

The latest development of low-noise readout ASIC in ATLAS allows acceptable signal-to-noise ratio above 10 at the end of life at 500 V of the operating voltage of the sensor. Accordingly, the specification of the maximum operating bias voltage is set to 500 V. The lower high voltage value, than 700 V e.g., has been beneficial, enabling higher yield for sensors. It matches the rating from the high voltage cables of SCT for possible recycling. The sensors are to be operated in a dry environment, at a typical sensor temperature range between -30 and -25 °C at the end of life, to reduce leakage currents.

The strips are AC-coupled and biased via polysilicon resistors. The default sensor biasing method is to set the n^+-implants at 0 V (grounded (GND)) and the backplane at negative high

[4] The current ATLAS strip sensors for LHC were fabricated in 4-inch wafer process. At the time, fabricating strip sensors in 6-inch wafer process had just become available. To date, fabricating strip sensors in 8-inch wafer process is still premature. We have chosen 6-inch wafer process for the ATLAS18 sensors for its established reliability.

voltage[5]. This is to keep the voltage across the AC coupling to the minimum, given that the inputs to the readout electronics are close to ground potential.

Given a requirement of maximum 1% channel occupancy to ensure efficient and stable pattern recognition, ATLAS strip sensors for HL-LHC are sectioned into 4 or 2 rows of strip segments, with an approximate strip length of 2.4 cm in the inner and 4.8 cm in the outer radial part in the barrel section, respectively. With a strip pitch of 75.5 µm, occupancies are estimated to be 0.92% and 0.57%, respectively, at a pile-up of 200 events.

2.1 Barrel sensors: ATLAS18SS and ATLAS18LS

The barrel sensors with 4 or 2 strip segments are referred to as "short strip" (ATLAS18SS) or "long strip" (ATLAS18LS) sensors, respectively. The ATLAS18SS and LS sensors have inherited the features of the successful ATLAS17LS design, including utilization of the maximal allowed wafer area, strip pitch of 75.5 µm, chip boundary markers, two dicing lines[6] (the "inner cut" with an edge space of 450 µm in the longitudinal direction and 550 µm in the lateral direction to the strips and the "outer cut" of ∼1 mm in both directions), etc. The ATLAS18SS and LS sensors are diced along the inner cut lines (we refer to it as a "slim edge" design). A schematic layout of the ATLAS18SS sensor is shown in Fig. 2, together with an expanded view of the fiducial markers (cf. Fig. 2a for the locations and Fig. 2b for the shapes).

The new features in ATLAS18SS and LS designs with respect to the last ATLAS17LS design are:

- optimizations of shapes and locations of fiducial marks (-105 µm and -100 µm from the nominal lateral and longitudinal cut edge, respectively, to expand the minimum metal width to 10 µm to avoid over-etching. They were -95 µm in the ATLAS17LS layout.)
- addition of a fiducial mark M, which is a comparable pattern to the mark G but with four squares inside instead of four circles, to allow usage of a pattern recognition program which prefers straight line rather than circle. (There was no mark M in the ATLAS17LS layout.)
- the layout of miniature sensors and test structures in the halfmoons (cf. Section 3).

Specifications of the mechanical parameters are summarized in Table 1. The outer dimensions and areas are also listed in Table 3, together with those of the endcap sensors. In Table 1, the parameters are grouped with according to their characteristics where each group specifies

- Outer dimension – size (in x and y) with a tolerance to the dicing precision, thickness, uniformity, and flatness.
- Outer edge – edge space required to hold the reverse bias voltage between the bias-voltage ring and the cut edge, edge chipping and cracks for quality of dicing. The

[5]The voltages in this document are in the absolute values unless explicitly noted.

[6] The feature was first introduced in the ATLAS12 design to try reducing the dead area due to the edge space. The width of the outer cut was the default at the time, as adopted in the ATLAS strip sensors for LHC. Little disadvantages have been observed due to the inner cut dicing[4, 6–8]. The idea behind keeping two dicing lines is to make minimal changes to the successful designs and still to be prepared for un-expected events.

(a) Layout of the ATLAS18SS sensor. The triplet of Mark I fiducial markers is the stereo fiducial markers corresponding to Type 3 in Fig. 1a.

(b) Fiducial markers of the ATLAS18 main sensors.

Fig. 2: Schematic layout of the ATLAS18SS sensor and the fiducial markers.

Table 1: Mechanical parameters of the barrel sensors.

Parameter	Description	Specification (*1)
Outer dimension		
Width×Length	Width: lateral, Length: longitudinal to the strip direction, with tolerance to dicing	(97950 ± 20)×(97621 ± 20) μm^2
Thickness	physical thickness, with tolerance	320 ± 15 μm
Thickness uniformity	tolerance to uniformity of thickness over full area	± 10 μm
Flatness	tolerance to warpage over full area, unstressed	<200 μm
Outer edge		
Lateral×Longitudinal distance	distances from the inner edge of bias ring to the cut edge (after dicing), with tolerance to dicing	(550 ± 20)×(450 ± 20) μm^2
Edge chipping and cracks	mechanical damage to outer edge, after dicing	<40 μm inward
Strip segments:		
No. of rows	of strip segments	4 (SS) or 2 (LS)
No. of readout strips	per row	1280
Total No. of strips	per row, number of "readout" strips + 2 "field-shaping" strips (*2)	1282
Strips:		
Pitch	of strips	75.5 μm
Width of Implant	of strips	16 μm
Width of AC metal	of strips, aluminum metal (pure-Al), capacitively coupled (AC) over n-implant strips	22 μm
AC pad	on strip metal for probing and wirebonding	56×200 μm^2
DC pad	island of metal, directly connected to implant for probing implant	50×60 μm^2
Bias resistor	providing bias potential to strip implant, isolating adjacent strips	Polysilicon wiggling over the strip implant
Isolation structure	cutting off inversion layer on surface of silicon, surrounding n-strip implants continuously	narrow p-implant trace 6 to 8 μm wide
PTP structure	Punch-through protection structure, a narrow gap between the bias rail and the end of strip implant, protecting AC coupling capacitor from over-biasing	≤20 μm covered with a field-plate extended from the bias rail
Strip identifier	markers for visual identification of strip sequence, at every 10th, 50th strips, and the first readout strip (1) and the last readout strip (1280)	dot (•) marker at every 10th, numbers (e.g., 50) at every 50th, readout strip number at first and last readout strip
Chip boundary marker	small pads next to the AC pads, indicating 1st and 128th channel for those of each ASIC	30x36 μm^2
Bias-voltage pads:		
Bias ring	a pad contacting bias ring implant, along the AC pad rows of 1A and 4B (*3)	80×550 μm^2
Backplane	whole area contacting the backplane implant	whole area, Al-metalized
Edge ring	a pad contacting the edge ring implant, along the AC pad rows of 1A and 4B	80×550 μm^2, with an offset to the bias ring pads, avoiding aligning of the pads
Metal quality (wirebonding pads):		
Pull test mean	mean value of pull force to break wire-bonding, corrected for wire angle	> 10 g
Pull test RMS	RMS value of pull force to break wire-bonding	< 10% of mean
Probability for lift-off	fraction of breakage by peeling off from pad	<20 %
Fiducial markers:		
Minimum metal width	width of finished object	10 μm
Alignment to other marks	general tolerance to spatial precision of features on top surface	3 μm

(*1) Dicing at the "inner cut" lines (="slim-edge" dicing)

(*2) One extra strip outside of the first and the last readout strip, with its AC pad connected to the ground, to shape the electric field of the readout strips

(*3) cf. Fig. 2

edge space, in turn, defines the area with strips (which we refer to as "strip" or "active" area).

- Strip segments – number of rows of strips, number of "readout" and "total" strips in each row. The "readout" strips are to be connected to readout ASICs. The "total" number includes them plus one extra strip on each side of the first and the last readout strips. We refer to the extra strips as "field shaping" ones[7]. The rows of AC pads of the strip segments are labeled from 1A to 4B in the case of SS sensor as shown in Fig. 2a. The 1st digit corresponds to the row number (1-4) and the 2nd indicates the strip-end side (A-B).
- Strips – specification of a strip: strip pitch, widths of implant and AC-coupling metal, bias resistor, isolation structure, punch-trough protection structure (PTP), strip identifier, and chip-boundary marker.
- Bias-voltage pads – sizes of pads in the bias ring along the rows of strips, backside of the sensor, and edge ring.
- Metal quality – of the pads for wirebonding which is defined by the mean, r.m.s, and lift-off of the metal.
- Fiducial markers – minimum metal width for visibility, and general alignment tolerance to the spatial precision of features on top surface.

2.2 Endcap sensors: ATLAS18R0, ATLAS18R1, ATLAS18R2, ATLAS18R3, ATLAS18R4, ATLAS18R5

The endcap sensor, the "Stereo annulus" sensor, was first introduced in the ATLAS12EC/R0 design as a prototype of the inner-most R0 sensor [5]. The design is applied to six types of the ATLAS18 endcap sensors, R0 to R5, with optimizations of the layouts to fit in the petal geometry and allow for optimal coverage of the usable area of a 6-inch wafer.

The basic layout of an endcap sensor is defined based on the geometry shown in Fig. 3a. In the global polar coordinate system, the origin (O) is at the beamline of the ATLAS detector. The X and Y axes are set such that the Y axis is the radial axis along the strip direction passing through the center of the sensor and the X axis orthogonal to it[8]. For each sensor, the circles of the inner and the outer edges and the circle of the center of the sensor are defined by the radii, R_i, R_o, and R, respectively. The strips are laid out in a fan-out geometry with an angular pitch, φ_p. The focal point F is rotated by φ_s(20 mrad) about the center of the sensor (Ow) with respect to the Y axis in the global coordinate system. The focal point F is specific to the sensor in each radius, R. A schematic view of the strips is shown in (Fig. 3b). We refer to the feature as that the rotation angle is "built in the strips", instead of having the whole sensor rotated as in the barrel stave.

[7] They are to assure that the electric field of the 1st and the last "readout" strips is similar to that of other readout strips. Their AC-metals are to be connected to the ground potential of the readout ASICs to avoid sharing their signals with the readout strips.

[8] Conventionally, the polar coordinate system with the X and Y axes are referred to as the "global coordinate system".

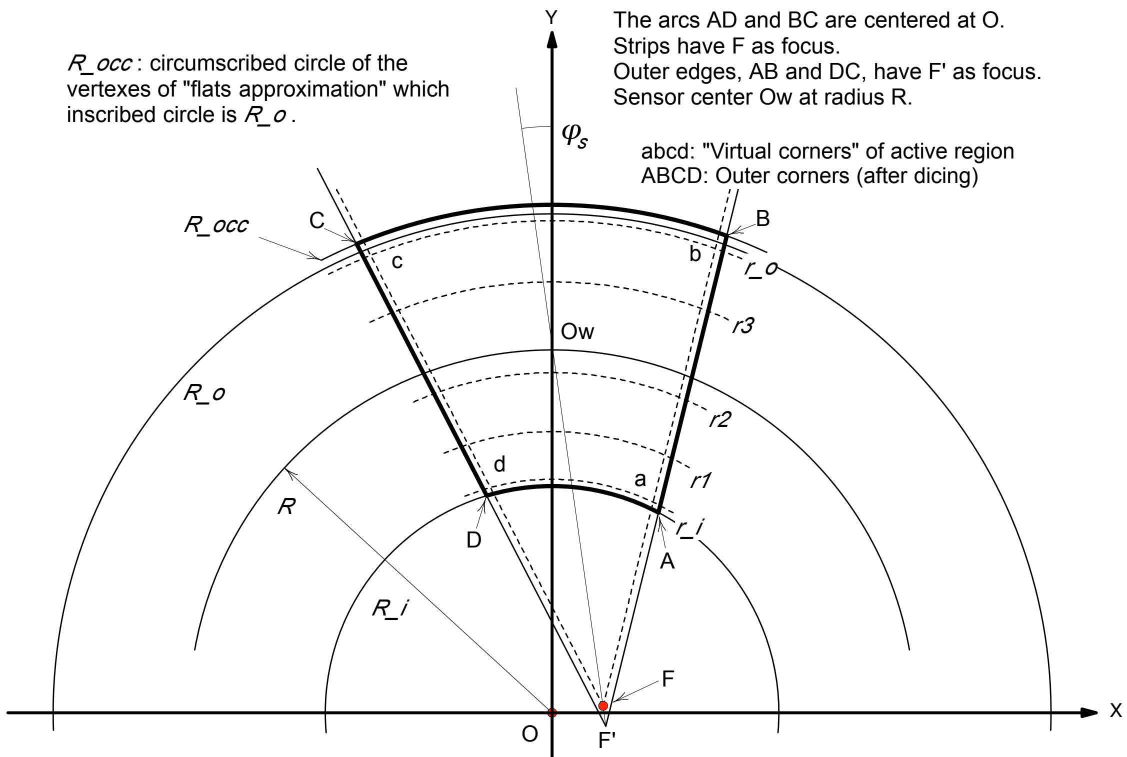

(a) Strips are rotated by angle ϕ_s around the center of the sensor (Ow), while the circles of the inner and the outer edges are kept centered at the origin (O).

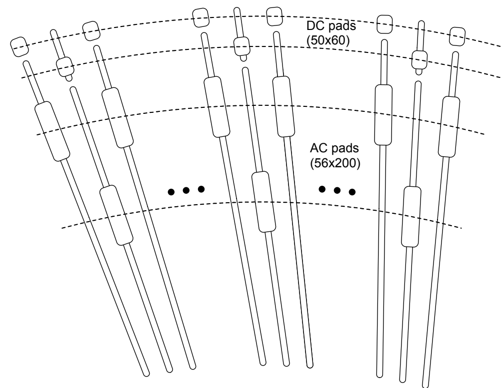

(b) Schematic circular placement of rows of AC and DC pads along their circles at the ends opposite to the polysilicon resistors. The pads are oriented along the directions of their strips.

Fig. 3: (a) Definition of dimensions of the endcap sensor and (b) the circular placement of rows of the probing pads.

The edge regions of the endcap sensors are laid out only with the inner-cut dicing line[9] (cf. the two dicing lines of the barrel sensor, Section 2.1). The longitudinal outer edges of the "sensor" are at the radii of R_i and R_o. The longitudinal boundaries of the "strip area" are set at the radii of r_i and r_o, 450 µm "inward" from the radii of R_i and R_o. The "lateral boundaries" of the strip area are set at half angular pitch outward from the first and the last strips. The corners of the "strip area" (a, b, c, and d in Fig. 3a) are defined by the cross points of the radii r_i and r_o and the "lateral boundaries" of the strip area. The lateral outer edges of the "sensor" are set parallel to the boundaries a-b and c-d, 550 µm outward. Thus, the focal point of the lateral outer edges, F′, has an offset from the focal point of the strips, F.

The longitudinal edges of the sensor are designed to be circular. To realize this in practice, the circular dicing is approximated by 16 consecutive short straight lines ("16 flats"). In order to keep the required space of the edge region, the circle of the inner edge is made with the circle R_i being the circumscribed circle of the flats. The circle of the outer edge is made with the circle R_o being the inscribed circle, thus, the vertexes of the flats are on the circumscribed circle, R_{occ}. The resulting radial extent of the endcap sensor is longer than the nominal length defined by R_i and R_o by 3 to 13 µm depending on the endcap sensors. The corners of the outer edges of the sensor are labeled as (A, B, C, D). The corners of the inner edge, A and D, are on the circle R_i, and the corners of the outer edge, B and C, are on the circle R_{occ}.

The basic parameters of the endcap sensors are summarized in Table 2 (cf. also Fig. 1c). The dimensions and areas are summarized in Table 3. The strip "angular pitch" is constant in each row of strips. The strip "pitch" varies along the radius. In Table 2, the strip "pitches" are calculated at the inner radii of the row of strip segments, r_i (Row0), r_1 (Row1), r_2 (Row2), and r_3 (Row3), which are the narrowest pitches of the rows[10]. The ATLAS18 endcap sensors have followed the features of ATLAS12EC/R0 and the ATLAS18SS barrel sensors. Those that are different from the barrel sensor are:

- Number of strips per strip segment, as listed in Table 2 and 3.
- Circular placement of rows of wirebonding and probing pads along their circles, and orientation of the pads along the directions of their strips. (Fig. 3b)
- Circular placement of the fiducial marks along their circles.

2.3 Fiducial markers of endcap sensors

The fiducial markers of the endcap sensors have followed the barrel sensors in Fig. 2. These markers are Mark E, F, G, H, I, and K, with their shapes as defined in Fig. 2b and arranged along the circles of their radii in fan-out geometry of Fig. 3a. The coordinates of fiducial markers of R0 to R5 sensors are summarized in Table 4.

The endcap sensors have special sets of fiducial markers, Type 1 to Type 3. Their overall function is similar to the "stereo fiducial markers" (Type 3 in Fig. 1a) in the barrel sensor. Their role is to align the sensors.

[9] This is due to two reasons: the layouts of the ATLAS18 endcap sensors started from scratch; the optimization to fit in the petal geometry and in the 6-inch wafer maximally has preferred the edge space only with the inner cut dicing.

[10] The "average" pitches can be calculated at the radii of the center of the strips by using the formulae in the Appendix A

Table 2: Parameters of the endcap sensors.

Basic parameters (in wafer coordinate)

Endcap sensor		R0	R1	R2	R3	R4	R5
a	x	39.0955	49.3763	36.7098	32.5878	38.4555	43.9394
	y	-56.1068	-47.3110	57.6942	-60.1220	-56.5475	-52.4005
b	x	47.3140	56.0569	-24.7238	36.0039	41.6635	46.9007
	y	47.5119	36.8121	62.5777	56.7436	52.5883	47.8989
c	x	-49.3826	-57.7362	-24.6016	-38.3392	-43.8444	-48.9050
	y	47.3061	36.6449	-63.8040	56.6286	52.4805	47.7996
d	x	-37.0270	-47.6970	36.5875	-30.2525	-36.2747	-41.9351
	y	-55.9010	-47.1438	-56.4678	-60.0070	-56.4397	-52.3012
A	x	39.6071	49.8880	37.2139	33.1240	38.9917	44.4755
	y	-56.6118	-47.8155	58.2059	-60.6002	-57.0256	-52.8785
B	x	47.8979	56.6409	-25.1307	36.5666	42.2263	47.4636
	y	47.9166	37.2181	63.1617	57.1708	53.0158	48.3267
C	x	-49.9845	-58.3384	-25.0056	-38.9200	-44.4253	-49.4860
	y	47.7066	37.0474	-64.4064	57.0531	52.9057	48.2253
D	x	-37.5210	-48.1909	37.0887	-30.7708	-36.7930	-42.4533
	y	-56.4013	-47.6446	-56.9616	-60.4823	-56.9153	-52.7770
	R_i (mm)	384.0500	489.3730	575.1440	638.1590	756.4510	867.0120
	R_o (mm)	488.8730	574.6440	637.6590	755.9510	866.5120	968.2350
	R_occ (mm)	488.8826	574.6553	637.6715	755.9547	866.5162	968.2397
	(dR_(occ-o))	0.0096	0.0113	0.0125	0.0037	0.0042	0.0047
	R_Ow (mm)	438.6140	534.6390	609.4050	697.8990	812.4710	918.7490
	r_i (mm)	384.5000	489.8230	575.5940	638.6090	756.9010	867.4620
	r1 (mm)	403.4810	507.9160	606.4020	664.8320	811.4820	907.6230
	r2 (mm)	427.4620	535.0090	---	697.0550	---	---
	r3 (mm)	456.4420	559.1010	606.4020	729.2780	811.4820	907.6230
	r_o (mm)	488.4230	574.1940	637.2090	755.5010	866.0620	967.7850
Strip parameters							
(*)No. Strips,	Row0	1026	1282	1538	898	1026	1154
	Row1	1026	1282	---	898	---	---
	Row2	1154	1410	---	898	---	---
	Row3	1154	1410	1538	898	1026	1154
Stereo angle φ_s (mrad)		20	20	20	20	20	20
Ang pitch φ_p (μrad),	Row0	193.0863	154.7122	129.0774	109.5053	96.1753	85.7429
	Row1	193.0863	154.7122	---	109.5053	---	---
	Row2	171.6880	140.6774	---	109.5053	---	---
	Row3	171.6880	140.6774	129.0774	109.5053	96.1753	85.7429
(**)Strip Pitch (μm),	Row0	74.4	76.0	74.5	70.0	72.9	74.5
	Row1	78.1	78.8	---	72.9	---	---
	Row2	73.6	75.4	---	76.4	---	---
	Row3	78.5	78.8	78.4	80.0	78.1	77.9
(***)Strip L (mm),	Row0	19.0	18.1	30.8	26.2	54.6	40.2
	Row1	24.0	27.1	---	32.2	---	---
	Row2	29.0	24.1	---	32.2	---	---
	Row3	32.0	15.1	30.8	26.2	54.6	60.2

Note:

R_o	Inscribed circle of flats of outer edge
R_occ	Circumscribed circle of flats of outer edge
r_x	Boundaries of strip area
(*)	"No. Strips" includes the field shaping strips.
	The 1st and the last "readout" strip are "1" and "No.Strips" - 2.
(**)	Calculated at the inner radius of the boundaries of the row
(***)	Calculated from the inner to the outer radius of the boundaries of the row

Table 3: Dimensions and areas of the ATLAS18 sensors.

	SS	LS	R0	R1	R2	R3	R4	R5
Dimension(*1)								
- Width(*2) (mm)	97.951	97.951	97.882	114.979	127.568	75.487	86.652	96.950
- Length(*2) (mm)	97.621	97.621	106.879	87.831	65.480	118.655	111.070	102.369
- Thickness(*3) (mm)	0.320	0.320	0.320	0.320	0.320	0.320	0.320	0.320
Sensor area(*1)								
- Area (mm^2)	9562	9562	9189	9100	7601	8213	8943	9311
- Perimeter (mm)	391	391	385	384	368	375	383	387
Strip area(*4)								
- Area (mm^2)	9368	9368	8996	8912	7424	8018	8744	9110
- Perimeter (mm)	387	387	381	380	364	371	379	383
- Strip segments	4	2	4	4	2	4	2	2

(*1) Outer dimension of sensor. The maximum values in the endcap sensors.
(*2) Width and Length are lateral and longitudinal directions to strips, respectively
(*3) Nominal thickness
(*4) Inside of the bias ring

- "Type 1": These are located in the lateral edge regions of the sensor, on a circle of pre-defined radius from the center of sensor in the global coordinate system, to help positioning the sensor on the petal face. The markers are Mark I with the longer side along the lateral edge of the sensor with a letter "R" associated in the mask, to differentiate from other Mark I markers being used as "Type 3". We refer to the marker as "Mark I_R".
- "Type 2": These are located in the lateral and the longitudinal edge regions, to define the center of sensor (Ow) by the crossing point of lines across a diagonal pair of the markers. The markers are Mark K with the longer side along the edge. We refer to those in the longitudinal edges as "Mark K (h)" and to those in the lateral edges as "Mark K (v)".
- "Type 3": Three Mark I markers are placed on each of the longitudinal edges to help align the sensors along the radial axes on the petal face. In the inner three sensors of R0 to R2, each markers are on their axes. The outer three sensors of R3 to R5 are made of a pair of the sensors. In the left of sensors R3 to R5, their two right markers are to align with the left and center markers of R0 to R2 sensors, while in the right of sensors R3 to R5, their left markers are to align with the right markers of R0 to R3. Their lines of axes and the markers are shown graphically in Fig. 1b.

3 Wafer layouts

3.1 Wafer layouts of ATLAS18 sensors

We have fitted one large-format main sensor in the center of the wafer. In the remaining space outside of the main sensor, referred to as "halfmoons", we have laid out miniature sensors and test structures. The final layouts of the two barrel wafers (SS and LS) are shown in Fig. 4 and the layouts of the six endcap wafers (R0 to R5) in Fig. 5. In the main sensors, the dotted lines indicate the boundaries of the strip rows. The identification label and scratch pads as described in Appendix C are implemented to identify the wafer number and the individual pieces such as the main sensor, halfmoons, miniature sensors, test structures, etc.

Table 4: Fiducial markers of the ATLAS18 endcap sensors.

R-sensor		R0		R1		R2		R3		R4		R5	
Type	Marker	X (mm)	Y (mm)	X (mm)	Y (mm)	X (mm)	Y (mm)	X (mm)	Y (mm)	X (mm)	Y (mm)	X (mm)	Y (mm)
Type 1	Mark I_R	43.8180	-2.1942	53.3679	-2.6703	3.0423	60.8171	34.7653	-0.8664	40.5331	-1.0117	45.8983	-1.1472
	Mark I_R	-43.9036	-2.2028	-53.4723	-2.6808	3.0543	-60.9363	-34.7989	-0.8681	-40.5726	-1.0137	-45.9427	-1.1494
Type 2	Mark K (h)	0.0000	50.1590	0.0000	39.9050	-28.1540	0.0000	0.0000	57.9520	0.0000	53.9410	0.0000	49.3860
	Mark K (h)	15.9016	49.9003	14.6709	39.7177	-28.0035	13.8530	14.8020	57.8070	14.3145	53.8227	13.9558	49.2854
	Mark K (h)	-15.9016	49.9003	-14.6709	39.7177	-28.0035	-13.8530	-14.8020	57.8070	-14.3145	53.8227	-13.9558	49.2854
	Mark K (h)	0.0000	-54.4640	0.0000	-45.1660	34.1610	0.0000	0.0000	-59.6400	0.0000	-55.9200	0.0000	-51.6370
	Mark K (h)	-17.4827	-54.8620	-16.7898	-45.4540	34.4130	-17.0237	-15.3185	-59.8239	-14.9114	-56.0670	-14.6568	-51.7609
	Mark K (h)	17.4827	-54.8620	16.7898	-45.4540	34.4130	17.0237	15.3185	-59.8239	14.9114	-56.0670	14.6568	-51.7609
Type 2	Mark K (v)	47.2583	41.1786	56.0006	30.4804	-18.3941	62.5211	36.2644	50.4137	41.9224	46.2589	47.1595	41.5702
	Mark K (v)	-49.0752	40.9977	-57.4283	30.3381	-18.2969	-63.4959	-38.3473	50.3110	-43.8512	46.1635	-48.9113	41.4834
	Mark K (v)	-39.9953	-34.8500	-50.5003	-27.4866	17.4211	-59.2140	-31.7946	-44.1999	-37.7484	-41.6532	-43.3612	-38.2221
	Mark K (v)	41.2582	-34.4673	51.4226	-27.1654	17.2006	59.6916	33.5055	-43.9586	39.3456	-41.4204	44.8101	-38.0050
Type 3	Mark I	-8.9080	50.0778	-10.4712	39.8096	-28.0481	-11.6196	24.3122	57.5609	27.8510	53.4932	31.1249	48.8855
	Mark I	-1.7107	50.1560	-2.0109	39.9015	-28.1501	-2.2315	35.4342	57.1210	40.5998	52.9892	45.3706	48.3223
	Mark I	5.4870	50.1282	6.4498	39.8688	-28.1138	7.1572	-29.5997	57.3722	-33.9120	53.2771	-37.8976	48.6440
	Mark I	-7.0012	-54.5278	-8.9207	-45.2473	34.2565	-10.4839	20.5298	-59.9703	24.3195	-56.3110	27.8771	-52.0852
	Mark I	-1.3445	-54.4664	-1.7132	-45.1690	34.1645	-2.0133	29.9215	-60.3417	35.4518	-56.7511	40.6363	-52.5897
	Mark I	4.3125	-54.4882	5.4948	-45.1968	34.1972	6.4577	-24.9947	-60.1296	-29.6119	-56.4997	-33.9430	-52.3016
	Mark F	47.7595	47.7824	56.5023	37.0823	-24.9937	63.0232	36.4355	57.0358	42.0945	52.8803	47.3325	48.1907
	Mark F	-49.8397	47.5736	-58.1934	36.9126	-24.8695	-64.2612	-38.7829	56.9188	-44.2878	52.7708	-49.3488	48.0899
	Mark F	39.4910	-56.4616	49.7720	-47.6654	37.0639	58.0900	33.0007	-60.4562	38.8687	-56.8816	44.3527	-52.7345
	Mark F	-37.4105	-56.2523	-48.0804	-47.4955	36.9395	-56.8514	-30.6531	-60.3390	-36.6752	-56.7719	-42.3352	-52.6335
	Mark M	47.7556	47.4486	56.4984	36.7485	-24.6600	63.0192	36.4482	56.7023	42.1071	52.5468	47.3451	47.8572
	Mark M	-49.8226	47.2411	-58.1762	36.5801	-24.5371	-64.2440	-38.7823	56.5859	-44.2872	52.4379	-49.3481	47.7570
	Mark M	39.5397	-56.1323	49.8207	-47.3362	36.7346	58.1387	33.0328	-60.1249	38.9009	-56.5503	44.3849	-52.4032
	Mark M	-37.4724	-55.9242	-48.1423	-47.1675	36.6115	-56.9133	-30.6986	-60.0083	-36.7207	-56.4412	-42.3807	-52.3029
	Mark E	47.7690	47.6181	56.5118	36.9180	-24.8295	63.0327	36.4532	56.8722	42.1122	52.7167	47.3501	48.0272
	Mark E	-49.8428	47.4099	-58.1964	36.7490	-24.7059	-64.2643	-38.7941	56.7555	-44.2990	52.6075	-49.3600	47.9266
	Mark E	39.5263	-56.3018	49.8072	-47.5057	36.9041	58.1253	33.0279	-60.2948	38.8959	-56.7203	44.3800	-52.5732
	Mark E	-37.4522	-56.0931	-48.1221	-47.3363	36.7804	-56.8931	-30.6868	-60.1779	-36.7090	-56.6109	-42.3689	-52.4725
	Mark G	47.7022	46.7756	56.4449	36.0755	-23.9870	62.9657	36.4286	56.0274	42.0873	51.8719	47.3252	47.1824
	Mark G	-49.7424	46.5708	-58.0959	35.9098	-23.8667	-64.1637	-38.7357	55.9124	-44.2404	51.7644	-49.3013	47.0835
	Mark G	39.5931	-55.4592	49.8741	-46.6631	36.0616	58.1923	33.0526	-59.4500	38.9208	-55.8754	44.4049	-51.7284
	Mark G	-37.5527	-55.2539	-48.2227	-46.4971	35.9412	-56.9937	-30.7453	-59.3347	-36.7675	-55.7677	-42.4277	-51.6294
	Mark E	41.0394	-37.2256	51.2518	-29.3154	6.0365	60.5791	33.7987	-33.9267	40.5041	-2.0005	45.5699	-12.2707
	Mark E	-39.7267	-37.0935	-50.2928	-29.2191	6.0365	-60.5788	-32.5114	-33.8624	-40.5041	-2.0005	-45.1697	-12.2507
	Mark E	42.9360	-13.3138	53.3972	-2.3014			34.7406	-1.7103				
	Mark E	-42.5777	-13.2778	-53.5163	-2.3133			-34.7405	-1.7103				
	Mark E	45.2280	15.5817	55.3049	21.7200			35.6824	30.5055				
	Mark E	-46.0230	15.5018	-56.3828	21.6118			-36.9697	30.4413				
	Mark H	41.1023	-36.4328	51.3148	-28.5227	5.2438	60.6421	33.8220	-33.1318	40.5274	-1.2057	45.5933	-11.4759
	Mark H	-39.8212	-36.3040	-50.3873	-28.4296	5.2470	-60.6734	-32.5664	-33.0691	-40.5592	-1.2072	-45.2249	-11.4574
	Mark H	40.9765	-38.0183	51.1889	-30.1081	6.8292	60.5161	33.7755	-34.7215	40.4807	-2.7953	45.5464	-13.0655
	Mark H	-39.6322	-37.8830	-50.1982	-30.0086	6.8260	-60.4841	-32.4564	-34.6557	-40.4489	-2.7937	-45.1145	-13.0439
	Mark H	45.2908	16.3744	55.3678	22.5126			35.7057	31.3003				
	Mark H	-46.1175	16.2913	-56.4774	22.4012			-37.0247	31.2346				
	Mark H	45.1651	14.7890	55.2419	20.9273			35.6592	29.7107				
	Mark H	-45.9285	14.7123	-56.2882	20.8223			-36.9147	29.6481				

The “wafer coordinate” is defined such that the Y axis is along the primary wafer orientation flat and the X axis orthogonal to the flat. The strip direction of the main sensors is set along the Y axis, except in the ATLAS18R2 wafer. The strip direction of the ATLAS18R2 sensor is rotated by 90° to fit the shape in the wafer maximally[11].

3.2 Miniature sensors and test structures

Miniature sensors, test structures, monitor diodes, and other structures are laid out in the halfmoons. The miniature sensors are Mini (1×1 cm^2), SSmini (1×2.6 cm^2), and LSmini (1×5 cm^2) sensors. The test structures are the ATLAS test chips (TC, A1 to A4) and the vendor’s test structures (T1 to T4). The monitor diodes are the 1×1 mm^2 (MD1), 2×2 mm^2 (MD2), 4×4 mm^2 (MD4), 8×8 mm^2 (MD8), and 8×8 mm^2 with extra p-stop ring (MD8pstop). The other structures are the wirebonding test structures (WBTS) and the polysilicon bias resistor test structure (PRTS). The new structures implemented in the ATLAS18 wafer layouts are TC, MD8pstop, PRTS, and WBTS. The miniature

[11] The wafer coordinates coincide with the global coordinates (cf. Section 2.2) in general, but they are rotated by 90° in the ATLAS18R2 sensor.

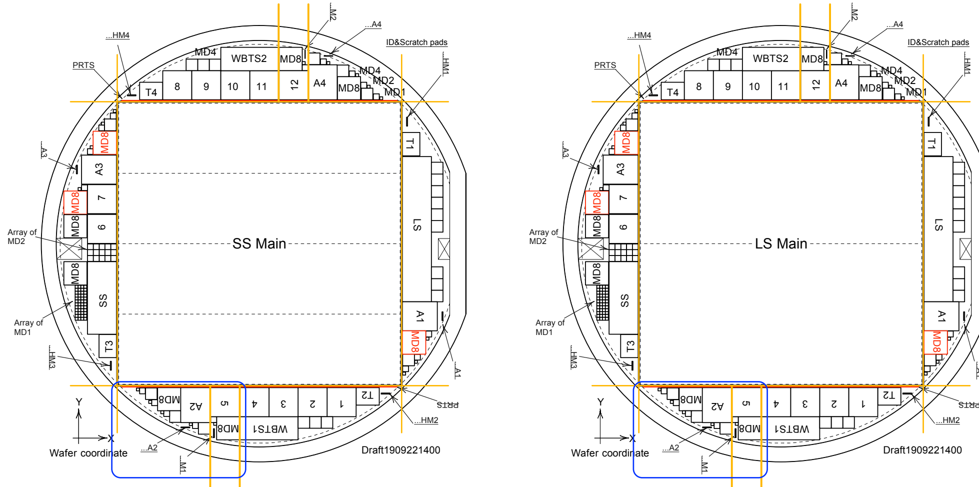

Fig. 4: The final wafer layouts of the ATLAS18 barrel sensors, SS and LS, in 6-inch wafers. Miniature sensors and test structures are laid out in the halfmoons. The orientations of minis and other pieces in the halfmoons are shown by the orientation of the numbers. MD8s in red are those with p-stop separation ring (cf. Fig. 6). Two QA pieces ("Mini&MD8" and "Testchip&MD8") enclosed in blue are diced out through the dicing lines in orange, under the "production-style" dicing.

sensors (Mini, SSmini, and LSmini) and the monitor diodes (MD8 etc.) have been described in the ATLAS17LS publication [6], and the ATLAS test chip (TC) in [9].

The MD8pstop diodes are identical to the MD8 with an extra p-stop ring between the diode pad and the guard ring (Fig. 6). These are designed to study the radiation damage effect more precisely. The extra p-stop ring isolates the currents that flow in the diode area from the edge region, thus defining the diode volume better. The locations of the MD8pstop diodes in the wafers are shown with a color (red) in Fig. 4 and 5.

All pieces in the wafers are arranged such that they can be diced out individually. For dicing out test structures for the quality assurance (QA) program, we have set two major dicing lines (orange color) in two halfmoons, as shown in Fig. 4 and Fig. 5 for the barrel and the endcap wafers, respectively. One test piece contains an ATLAS test chip and a MD8 diode (Testchip&MD8) and the other a Mini sensor and a MD8 diode (Mini&MD8). We refer to these test pieces as "QA" pieces. No MD8pStop diode is included in the QA pieces[12]. For the large scale production, only the QA pieces in one halfmoon of every wafer are diced out, shown enclosed in blue in the corresponding halfmoons in Fig. 4 and Fig. 5. We refer to the dicing scheme of the large scale production as "Production-style" dicing.

The PRTS is a straight-line structure, spanning the full width of the wafer next to both ends of the main sensor, with sets of 10 daisy-chained copies of polysilicon resistors (DS10) (Fig. 7). When a dicing line crosses the structure, the line and the boundary of DS10 are arranged such that the line is at the end of DS10 and the daisy-chain is terminated with a set of 9 resistors (DS9). The purpose of the structure is to monitor the polysilicon process in the endcap sensors (R0 to R5) to

[12]The QA pieces are to monitor the process quality, especially of the main sensors. The main sensor is designed without the extra p-stop ring to have the best breakdown performance.

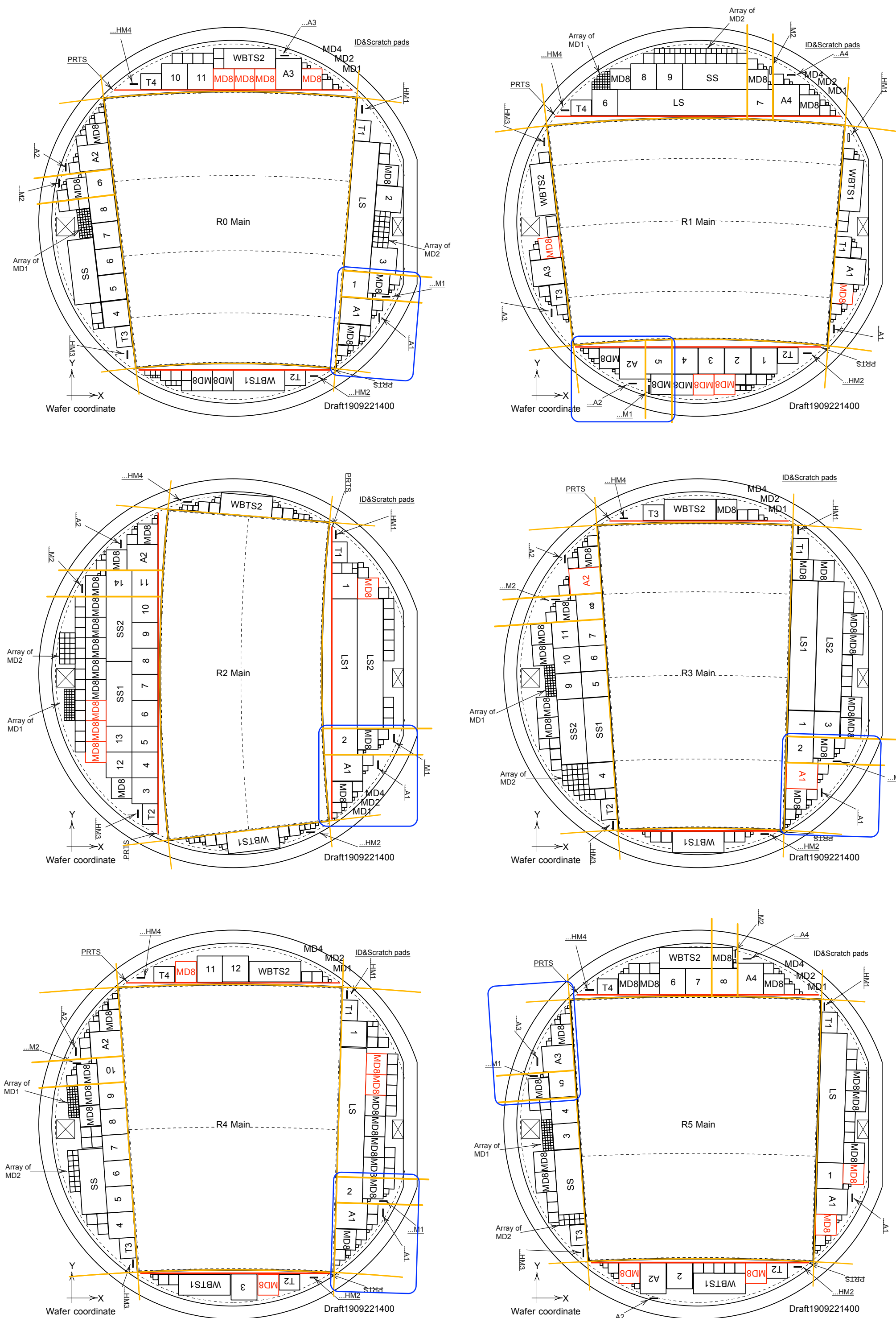

Fig. 5: The final wafer layouts of ATLAS18 endcap sensors, R0, R1, R2, R3, R4, and R5, in 6-inch wafers. Miniature sensors and test structures are laid out in the halfmoons, following the patterns in the barrel wafers (cf. Fig. 4). Two QA pieces ("Mini&MD8" and "Testchip&MD8") enclosed in blue are diced out through the dicing lines in orange, under the "production-style" dicing.

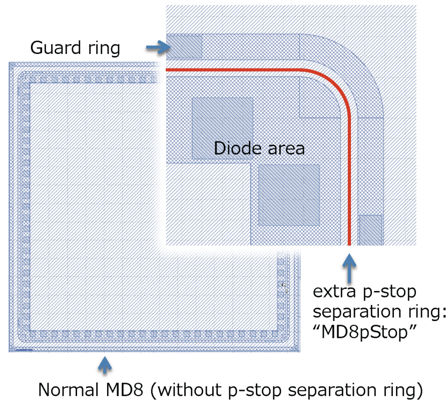

Fig. 6: MD8 diode with extra p-stop ring (MD8pStop).

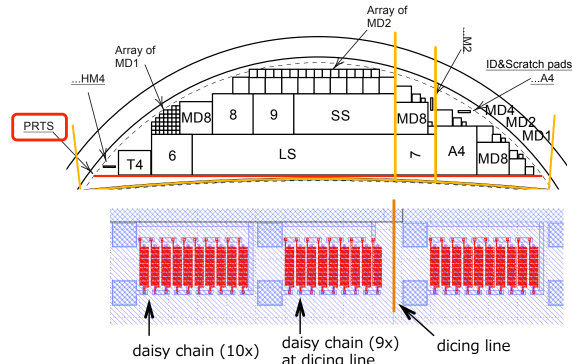

Fig. 7: Polysilicon Bias Resistor test structure (PRTS) in wafer R1.

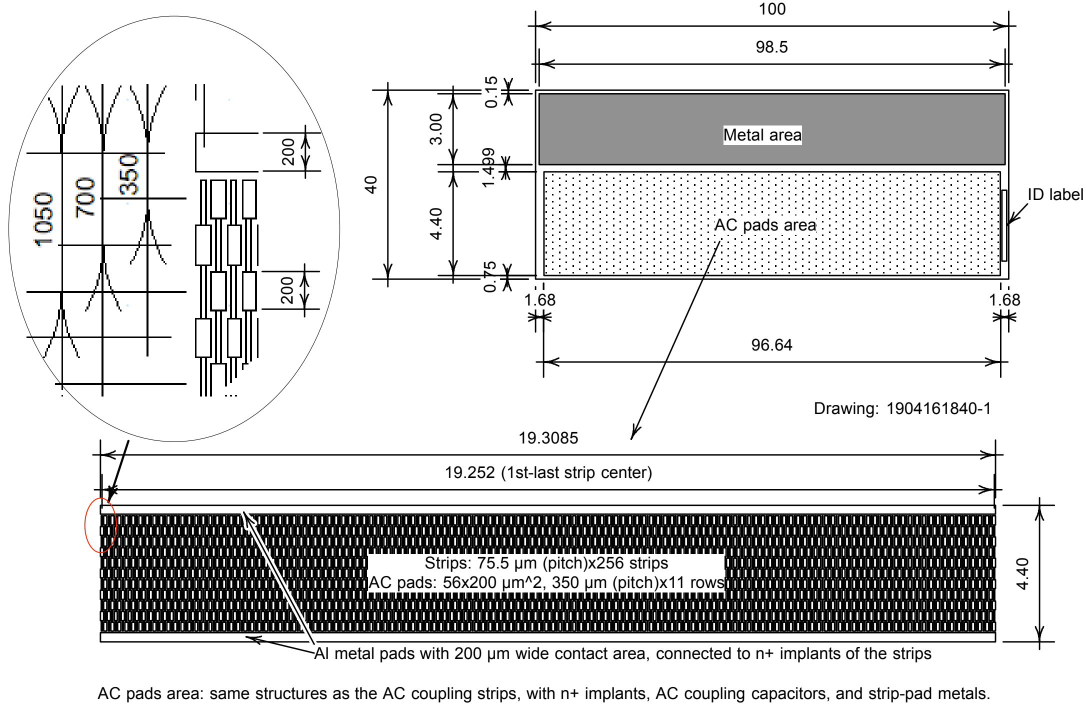

Fig. 8: Wirebonding test structure (WBTS).

complement the direct measurement of the polysilicon resistors of the strips (cf. Section 4.2). The PRTS is implemented in all layouts (SS, LS, R0 to R5).

The WBTS (Fig. 8) is designed to provide a test piece for wirebonding, with an area of a wide common metal pad (Metal area) and an area of strip structures with wirebonding pads (AC pads area). The AC pads area is made of the same strip structures as in the main sensor, i.e., n^+-implant, AC-coupling, Al-metal, and wirebonding pads, in each strip. The n^+-implant strips are connected to the common metal pad. The Metal and AC pads areas can be used for practice and tuning of wirebonding, as well as for verifying the quality of the metallization of the wirebonding pads (cf.

Table 1). The AC pads of the strips can be used for tuning the wirebonding parameters with an evaluation of damage to the structure through an electrical continuity test to the common pad. The number of wirebonding pads is maximized in the structure area, so that the evaluation can be made statistically.

4 Electrical Properties

4.1 Electrical properties common to all types of sensors

Electrical properties common to all sensor types are summarized in Table 5, classified into three blocks: wafer, sensor, and strips. We have adopted the p-type silicon as the wafer material for radiation tolerance, <100> crystal orientation for smaller Si-SiO_2 interface charge density, an oxygen concentration of 10^{16} to 10^{17} atoms/cm^3 for radiation-damage suppression, and the active thickness tolerance of >270 µm with an expected mean value of 290 to 300 µm. In the sensor block, we have specified maximum operating voltage of 500 V, breakdown voltage of > 500 V, leakage current and collected charge evaluated at 500 V, and the number of "bad" strips. The "collected charge" is the most probable value (MPV) of the collected charge signal distribution. The "bad" strips are those which have failed the properties in the strip block. In the vendor tests, they are identified from dedicated measurements (cf. the strip block in Table 6).

The values of the properties are specified before and after irradiation (cf. Section 2). They are listed in the columns of "Initial condition" and "Post-irradiation". In the Post-irradiation column, the properties are shown with an "arrow" if they are to be maintained the same as in the initial condition. They are shown with a new value and/or condition if they have a different specification.

We use a formula of temperature dependence of the current generated in silicon bulk [10], with an activation energy of 1.21 eV, for normalizing temperature variation.

4.2 Tests carried out by vendor

Before the delivery of the sensors, the vendor performs tests against the specifications in Table 1 and 5 to ensure the initial condition product quality. The test items are summarized in Table 6. The test items are in two blocks: Overall and Strips. In Overall, Visual inspection is to verify improper mechanical features such as edge chippings and scratches; Electrical tests is to verify properties such as full depletion voltage (V_{fd}) and breakdown voltage (V_{bd}), through the measurements of the overall capacitance ("body" capacitance) and the leakage current of the sensor as a function of bias voltage (C-V and I-V measurements), respectively, and Polysilicon resistance with the vendor's test structure.

In Strips, Visual inspection is to check for abnormal patterns; Electrical tests with a single probe on the wirebonding pad in each strip ("single-probe AC test") are to find such features as AC coupling dielectric "short"(Pinhole), AC metal "shorts" to neighbors (Short), AC metal "open" of shorter metal length due to a breakage in each strip (Open); and tests with the DC pads in three strips each ("3-probe DC test") are to identify implant "shorts" and bias resistor "disconnection". Both AC and DC tests are performed with the other end of the connection to the silicon bulk.

The AC test (with 1-probe) is to be done both for the barrel and the endcap sensors. The DC test (with 3-probes) at the vendor is only performed for the barrel sensors, due to limitations in the

Table 5: Electrical properties common to all types of sensors.

Parameters	Initial condition (*1)	Post-irradiation (*2)
Wafer:		
Material	p-type Silicon, float-zone (FZ)	--
Crystal orientation	<100>	--
Resistivity	>3.5 kΩcm	--
Oxygen concentration	1.5x10^16 to 6.5x10^17 (atoms/cm^3)	--
Active thickness (tolerance)	>270 μm	--
Sensor:		
Full depletion voltage (*V_fd*)	<350 V	--
Breakdown voltage (*V_bd*)	>500 V	>500 V or *V_fd*+50 V
Maximum operating voltage	500 V (at sensor)	←
Leakage current	<0.1 μA/cm^2	<0.1 mA/cm^2
	at 500 V, RH<10%	←
Leakage current stability	<15% at 500 V, RH<10%, 24 hours, after temperature correction (*3)	←
Bad strips	≤8 consecutive, <1% per segment	←
Collected charge (MPV(*4))	>6350 electrons, at 500 V	←
Strip:		
Resistance of n-implant strip	<50 kΩ/cm	←
Resistance of AC-metal strip	<30 Ω/cm	←
AC coupling capacitance (C_AC)	>20 pF/cm, at 1 kHz	←
Polysilicon bias resistor (*R_b*)	1.5 ± 0.5 MΩ	1.8 ± 0.5 MΩ
Inter-strip resistance (*R_int*)	>10×*R_b*, at 300 V	← at 400 V
Inter-strip capacitance (*C_int*)	<1 pF/cm (*5), at 300 V to its nearest neighbors on both sides, at 100 kHz or 1 MHz (main sensor or mini sensor, respectively)	← at 400 V

Notes:
(*1) Initial condition: measured at room temperature (RT), normalized(*3) to +20°C
(*2) Post-Irradiation condition: irradiation to a fluence of 1.6x10^15 neq/cm^2 and an ionizing dose of 66 MRad, measured at (or normalized(*3) to) -20°C, after annealing of 7 days at +25°C (or 80 min. at +60°C)
(*3) *I*=*T*^2*exp(-*E_k*/2*k_B***T*), where *I*, *T*, *E_k*, *k_B* are current, temperature (in Kelvin), activation energy (1.21 eV), and Boltzmann constant
(*4) MPV: most probable value
(*5) Interstrip capacitance of the endcap sensors (fan geometry) can be compared with the barrel sensor by using a scaling formula, *C_2* = *f* • (ln(*d_1*/*a*)) / (ln(*d_2*/*a*)) • *C_1*, where *d_1* is the average pitch and *C_1* the measured capacitance of an endcap sensor, *d_2*=75.5 μm the pitch of the barrel sensor, *f*=1.07 a factor to account for the fan geometry and *a*=20 μm an effective strip width.

testing equipment in production line in the case of circular placement and small size of the DC pads (cf. Section 2.2 and Fig. 3b). The DC test for the endcap sensors is replaced by the electrical test on the PRTS structure.

The vendor provides datasheets with the test results in an electronic format. Each sheet is identified by the ATLAS Upgrade serial number (cf. Appendix B) and includes associated production batch and wafer numbers.

5 Pre-production of ATLAS18 sensors/wafers

In advance to the full production of the ATLAS18 sensors, the pre-production[13] of 1041 sensors/wafers was launched, corresponding to an amount of 5% of the quantity needed by the experiment, including anticipated losses. The specification and the ATLAS18 sensor layouts were reviewed in a formal review (Final Design Review) by the experts in the field including outside the ATLAS community. Subsequently an invitation to tender of the supply of Pre-production sensors was issued and the contract was awarded to Hamamatsu Photonics K.K. The CAD drawings of the

[13]These sensors are to be used for large-scale construction trial. They are not planned to be used in the experiment.

Table 6: Tests carried out by vendor.

Test item	Description	Data
Overall:		
Visual inspection	scratches, residues, defects (edge chipping)	(*1)
Full depletion voltage (*V_fd*)	kink point in 1/(*C*^2) in C-V measurement	(V)
Leakage currents	at *V_fd*+50 V, and 500 V	(μA)
Polysilicon bias resistance	upper, lower with a test structure on wafer	(MΩ)
Breakdown voltage (*V_bd*)	I-V slope (at *V_bd*) > 5x slope (<<*V_bd*)	(V)
Leakage current vs Bias voltage (I-V)	up to 700 V (20 V step, 1 to 10 sec delay at a step), and short stability test (to keep 30 sec at the last voltage with recording the current every 10 sec)	(V-A)
Strips:		
Visual inspection	NG(No Good) strips: Abnormal objects under passivation, Abnormal pattern of bias resistors	segment# - strip#
AC coupling dielectric "short"	short to implant (AC test: 1-probe test on AC pad), with a momentary test voltage of 100 V	segment# - strip#
AC metal: "shorts"	short to neighbor AC metals (AC test)	segment# - strip#
AC metal: "open"	smaller AC coupling capacitance (AC test)	segment# - strip#
Implant: "shorts"(*2)	short to neighbor implants (DC test: 3-probe test on neighbor DC pads)	segment# - strip#
Bias resistor "disconnection"(*2)	large resistance (>>1.5 MΩ) (DC test)	segment# - strip#
PRTS test(*3)	daisy chain continuity test	(*1)

(*1) Only those sensors passed are to be delivered
(*2) Only for barrel sensors
(*3) Only for endcap sensors

wafer layouts for production were laid out, according to the specification and through more than 6 iterations with ATLAS to refine the details of the sensor and the wafer layouts[14].

Together with the pre-production units, an additional small amount of the ATLAS18SS sensors was fabricated as a "prototype" submission. In this paper, we refer to the sum of the pre-production and the prototype units as "Pre-production". The Pre-production wafers were delivered to CERN and KEK. The main sensors and the halfmoons were distributed to the testing clusters to be used for establishing acceptance procedures and evaluating the performance of the main sensors (Quality Control (QC))[11]. The QA pieces were distributed to the testing sites of the quality assurance program[12, 13]. The quantities of the Pre-production wafers are summarized in Table 7, with their breakdown per sensor type and the distribution to the testing clusters. Each main sensor, halfmoon, and QA piece were scratch-marked in the relevant scratch pads (cf. Appendix C) by the vendor for identification and association with the datasheet.

Qualities of the delivered main sensors are reviewed and reported here "as produced" through the data supplied by the vendor. The evaluations by the ATLAS collaboration through the QA and the QC programs are to be reported separately elsewhere.

Leakage currents as a function of bias voltage ("I-V") – The leakage currents as a function of bias voltage for all ATLAS18 sensors in Pre-production are compiled in Fig. 9. They are broken down by sensor type in Fig. 10. Specifications relevant to the I-V performance (cf. Table 5 and 6) are the Breakdown voltage (V_{bd}) > 500 V, and the Leakage current < 0.1 μA/cm^2 at 500 V. This corresponds to approximately 10 μA for the whole sensor. The Breakdown voltage is defined where the slope of I-V is > 5 times the slope of I-V at low bias voltage ($\ll V_{bd}$). In the figures, a line is

[14]A set of drawings of surface metal layers of the wafers out of the production drawings can be retrieved from the CERN EDMS file server. Y. Unno et al., *ATLAS18 (SS, LS, Rx (x=0 to 5)) technical specification and gds files (HPK) for Pre-production*, CAD files dated August 6, 2019, https://edms.cern.ch/document/2781829/1, access restricted on request.

Table 7: Summary of number of ATLAS18 wafers under Pre-production.

		Reception sites and Testing clusters				
		CERN			KEK	CERN(*)
Stype	Total/Stype	Cambridge + QMUL	Prague	Vancouver + Carleton	KEK + SCIPP	Cambridge + QMUL
18SS	318	159			159	60
18LS	318	159			159	
18R0	45		20	25		
18R1	45		25	20		
18R2	45		20	25		
18R3	90		40	50		
18R4	90		60	30		
18R5	90		40	50		
Total	1041	318	205	200	318	60

Stype: Sensor type
Total/Stype: Breakdown of number of sensors per sensor type and the total
Reception sites and Testing clusters:
Breakdown Total/Stypes per "Reception site" of CERN and KEK, and "Testing cluster"
CERN(*): Additional "prototype" production, specific to a cluster

plotted at 500 V as a reference. The upper range of the vertical axis is 500 nA (per sensor) which is approximately 1/20 of the specification. One can make a few observations in the plots:

1. The level of leakage currents is very low, order of 100 to 200 nA per sensor at 500 V, which is equivalent to a resistance of 2.5 to 5 GΩ per sensor.

2. The sharp increases of leakage currents are seen only above 500 V, meeting the specification of the Breakdown voltage. A small number of sensors show soft increase of leakage currents below 500 V. These sensors are within the specifications for the slope change and the total leakage current at 500 V. They should be monitored closely in the QC program.

3. The behavior of leakage current is similar in all sensor types (Fig. 10a to 10h), except in ATLAS18LS sensors (Fig. 10b). There is a group of sensors with currents at the level of 200 nA. The group is made of a fraction of the sensors from one fabrication batch. They are not specific to a wafer ingot[15]. The origin of the difference has not been identified.

4. There are small bumps of leakage currents around 300 V, to a varying degree in all sensor types. The bump position is correlated with the full depletion voltage. The increase can be explained by the current generation at the ohmic-contact boundary of the silicon bulk (p-type) and the backside implantation (high density p-type layer) when the depletion has reached the boundary. The amount of the current could be influenced by the subtlety in the processing of the backside layer. Little correlation is found with the batch or the ingot.

Leakage currents at 500 V bias voltage – The distributions of leakage currents at 500 V, normalized to unit area, are compiled[16] in Fig. 11, plotted by sensor types. The distributions of

[15] This is a group of 22 sensors (wafer#143-164) out of 37 in the batch of VPX32418. The batch is made from the same ingot as several other batches.

[16] The binning of the histogram is made such that the entries are counted in the range of a bin being greater than and less than equal of the suffix of the bin. The 1st and the last bin include the overflow below and above the range of the bin, respectively.

the sensor types are aligned, with the caveat mentioned in the item 3 of the previous paragraph, indicating a controlled quality of the wafers and the semiconductor processing. There are tails towards larger currents in the ATLAS18SS and especially in the ATLAS18LS sensors. Those of ATLAS18LS sensors are partly made of the group of the large currents observed in the I-V plot of Fig. 10b. Other tails in the larger currents contain by sensors with soft increase of the currents.

Full depletion voltages (V_{fd}) – The distributions of the full depletion voltages V_{fd} are complied in Fig. 12. The majority of the sensors meet the specification of <350 V by a margin. There is a group of the sensors with V_{fd} of 340 - 350 V, which are close to the specification. They are found to be made from one specific ingot. Usage of the wafers from such ingot was discussed to be avoided in the full production.

Breakdown voltages (V_{bd}) – The distributions of the Breakdown voltages are compiled in Fig. 13. The sensors with no Breakdown up to 700 V are assigned the Breakdown voltage of 700 V. In the plot, the last bin of 700 V is scaled down to 1/10 of the entries. There is no sensor with V_{bd} <500 V, thus meeting the specification of the Breakdown voltage.

Fraction of bad strips per segment – The distributions of the fraction of the bad strips per segment are compiled in Fig. 14. The bad strips are those identified in the section of "Strips" in Table 6. The fraction of the bad strips is specified to be <1 % per row of strip segments. The bin width is chosen to be 0.08%, representing one bad strip out of 1282 strips in a single barrel sensor segment. The first bin is scaled down to 1/20 of the entries. Most of the sensors have no bad strips. Only a few sensors have 6 to 8 bad strips. The overall fraction of bad strips per sensor is 0.007% on average.

Out of the tests carried out by the vendor, the quality of the sensors "as produced" is judged to be excellent.

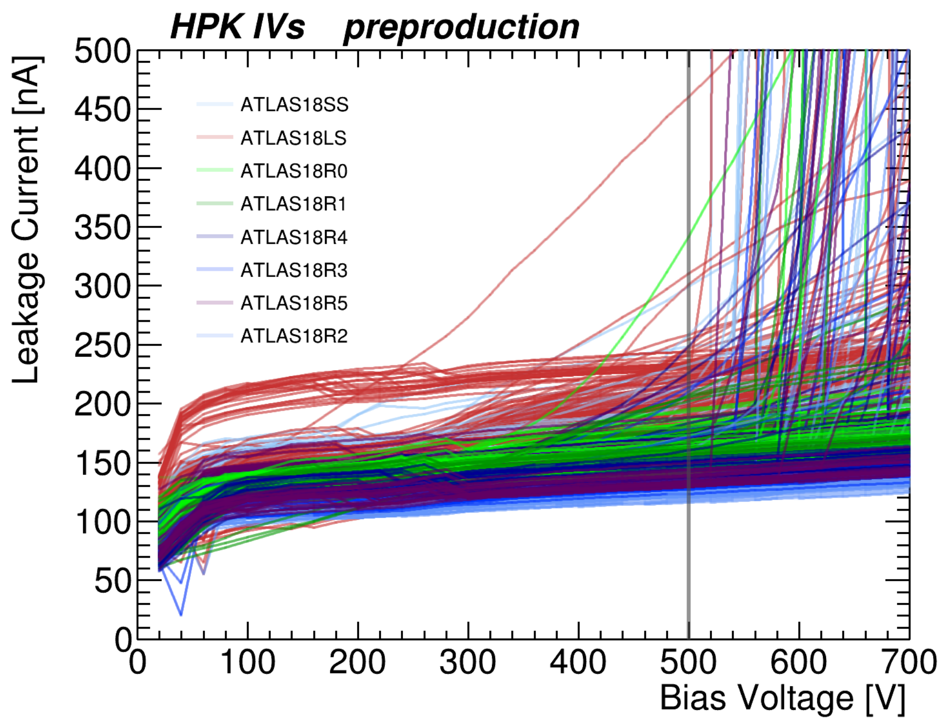

Fig. 9: Leakage currents as a function of bias voltage for all ATLAS18 sensors. The breakdown voltage is specified to be higher than 500 V. The leakage current at 500 V is to be below around 10 μA per sensor (see Table 5).

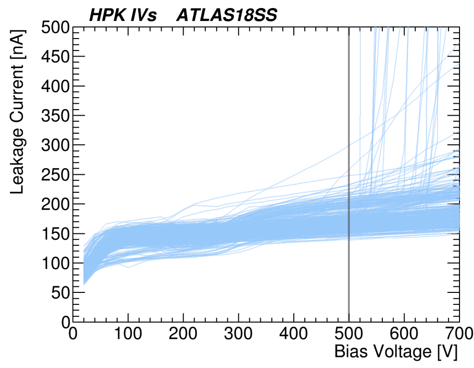

(a) Leakage currents of ATLAS18SS sensors.

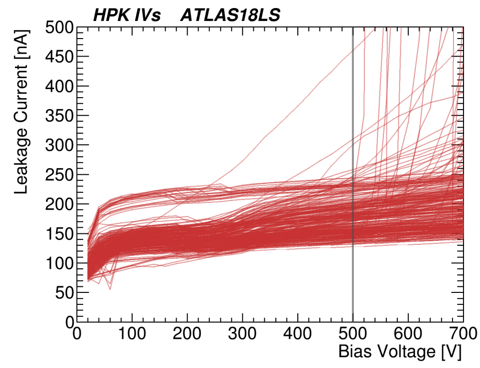

(b) Leakage currents of ATLAS18LS sensors.

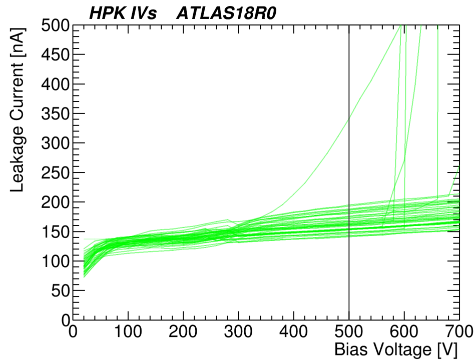

(c) Leakage currents of ATLAS18R0 sensors.

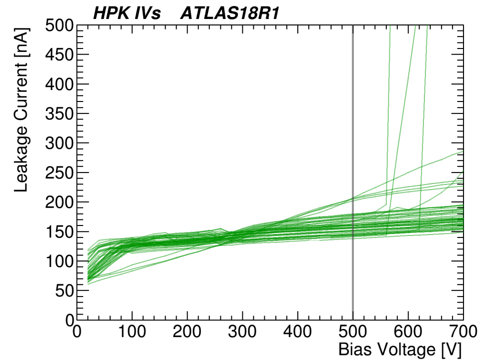

(d) Leakage currents of ATLAS18R1 sensors.

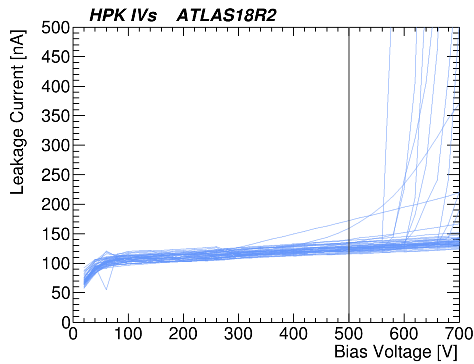

(e) Leakage currents of ATLAS18R2 sensors.

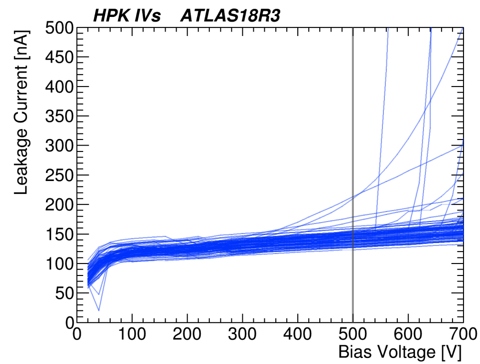

(f) Leakage currents of ATLAS18R3 sensors.

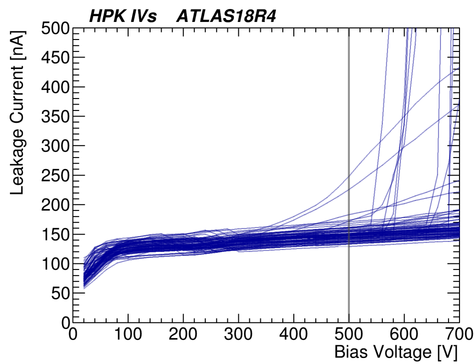

(g) Leakage currents of ATLAS18R4 sensors.

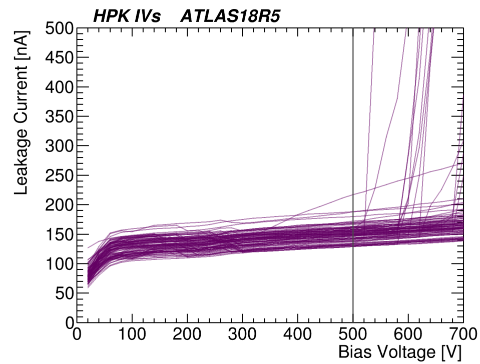

(h) Leakage currents of ATLAS18R5 sensors.

Fig. 10: Breakdown of leakage currents per ATLAS18 sensor type.

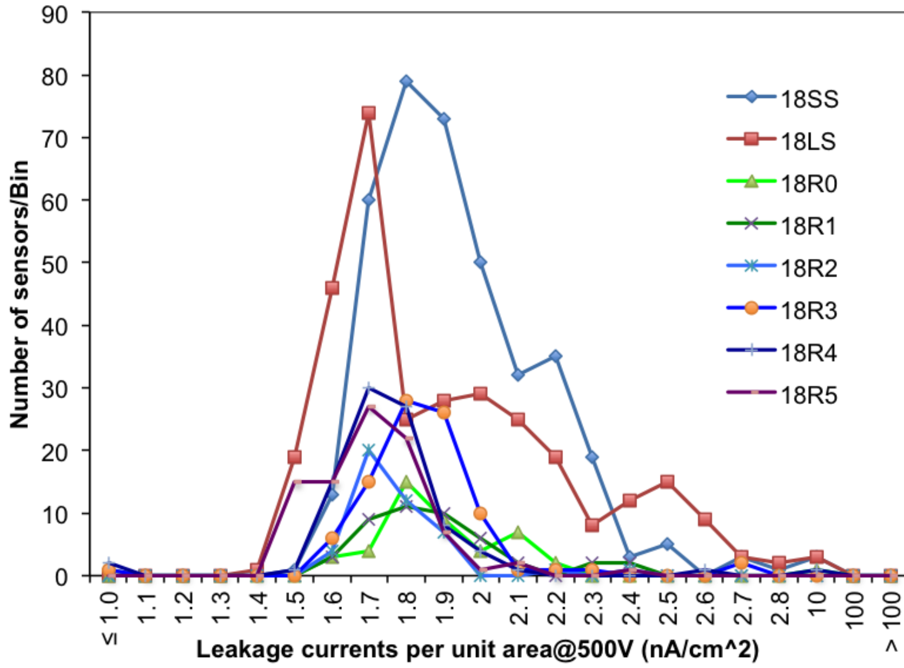

Fig. 11: Leakage currents per unit area at the bias voltage of 500 V plotted by sensor type. It is specified to be <100 nA/cm^2.

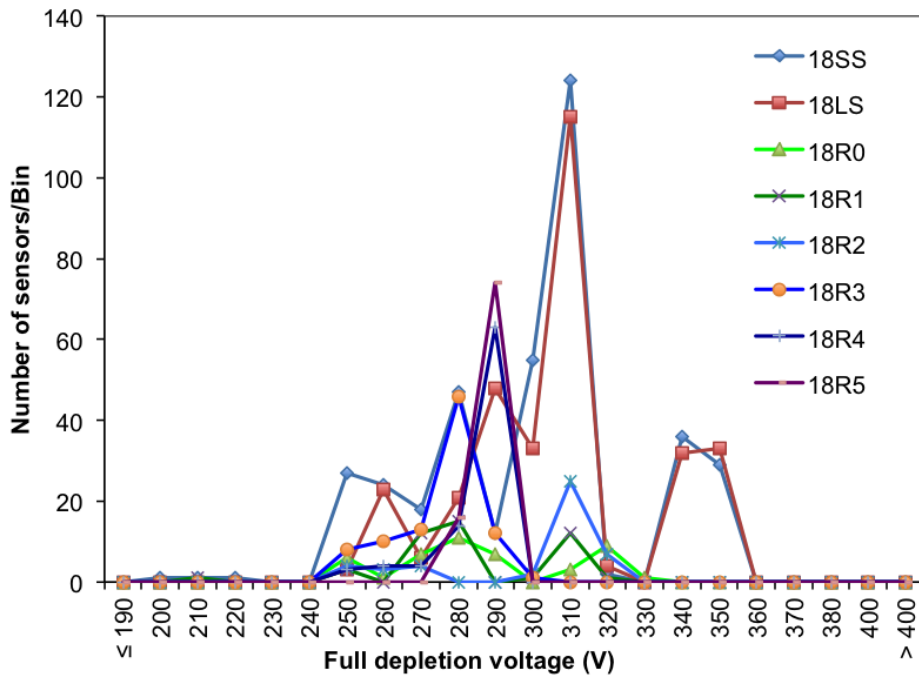

Fig. 12: Full depletion voltages (V_{FD}) plotted by sensor type, specified to be <350 V.

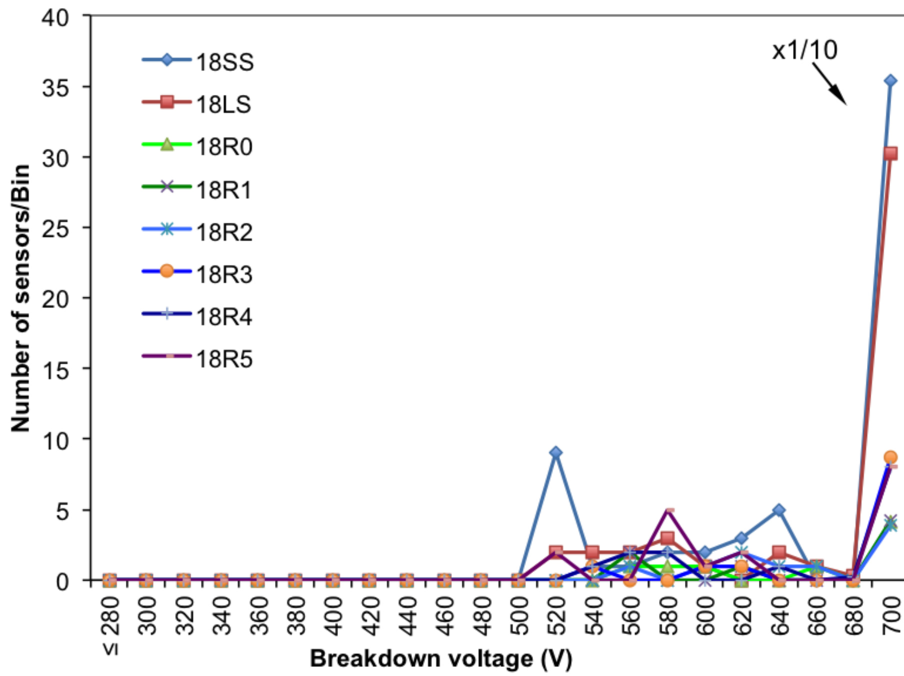

Fig. 13: Breakdown voltage (V_{BD}) plotted by sensor type, specified to be >500 V. All entries of the last bin of 700 V are scaled down to 1/10.

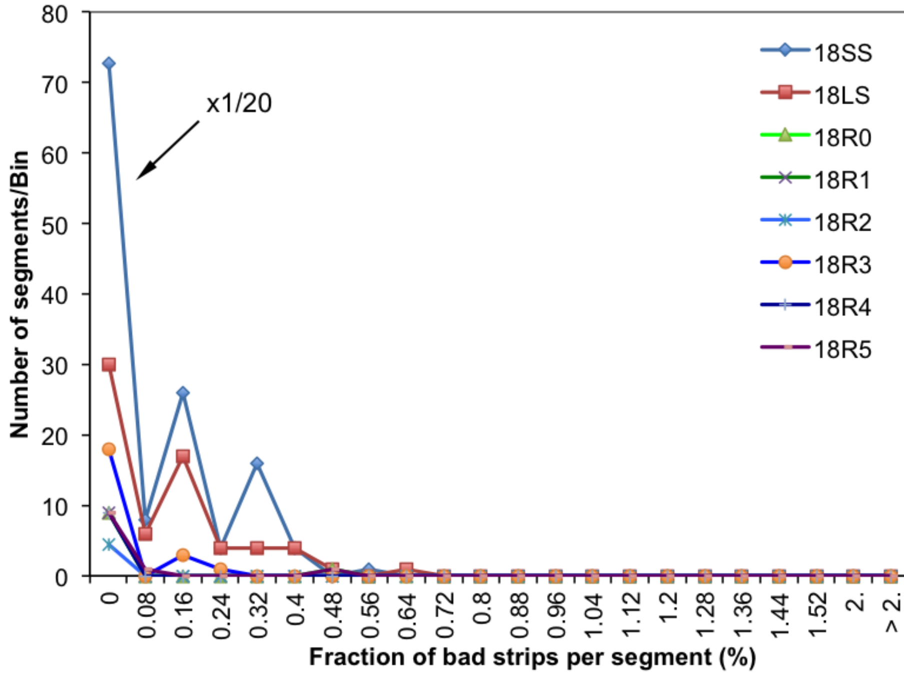

Fig. 14: Fractions of bad strips per strip segment plotted by sensor type, specified to be <1 % per segment. All entries of the first bin of 0 % are scaled down to 1/20.

6 Conclusion

The final design of the strip sensors for the Inner Tracker of the ATLAS upgrade, ATLAS18, is presented after a series of prototype iterations through many years of R&D. Eight different sensor layouts are defined, two for the barrel part, Short Strips (SS) and Long Strips (LS), and six for the endcap rings (R0 to R5).

The barrel sensors have rectangular shape with 4 or 2 rows of strip segments, utilizing the area of 6-inch wafer maximally. The endcap sensors have additional features of skewed-trapezoidal shape, strips in fan-out geometry with a built-in rotation angle, circular edges, as well as the requirement of six sensor layouts to fit in the petal geometry and in the area of 6-inch wafer maximally. New design optimizations have been introduced over the previous designs, ATLAS17LS and ATLAS12EC/R0. New structures have been laid out in the halfmoons such as the ATLAS testchip, monitor diodes with an extra p-stop ring, PRTS and WBTS. The final specifications of the sensors are defined to ensure that the sensors provide physics data efficiently throughout the entire lifetime of the experiment.

A pre-production of wafers corresponding to a 5% of the total production volume has been made to provide the final evaluation before proceeding to the full production. The performance has been reviewed and judged excellent from the test results measured by the vendor for this delivery.

A Formulation of the strips of the endcap sensors

In the geometry of Fig. 3a, the coordinates of i-th strip at a radius r are defined by

$$\begin{aligned} x(i,r) &= -r'\sin(\varphi_i' + \varphi_s) + R\sin(\varphi_s) \\ y(i,r) &= r'\cos(\varphi_i' + \varphi_s) - R\cos(\varphi_s) \end{aligned} \tag{A.1}$$

where

$$\begin{aligned} \varphi_i' &= (-1)(i - N/2 + 0.5)\varphi_p \\ b &= -2(2R\sin(\varphi_s/2))\sin(\varphi_s/2 + \varphi_i') \\ c &= (2R\sin(\varphi_s/2))^2 - r^2 \\ r' &= (-b + \sqrt{b^2 - 4c})/2\,. \end{aligned} \tag{A.2}$$

with N being total number of strips, i-th strip in clock-wise counting, φ_p angular pitch, φ_s rotation angle, and R radius of the wafer center of the sensor Ow. The basic parameters such as N, φ_p, φ_s, and R are summarized for each endcap sensor in Table 2. The coordinates of the ends of strips are calculated at the boundaries, r_i, $r1$, $r2$, $r3$, and r_o, of the rows of each endcap sensor.

B ATLAS Upgrade serial number

To identify a piece in the experiment, an ATLAS Upgrade serial number can be assigned to the object. The ATLAS Upgrade serial number scheme is made of 14 digits of alpha-numeric code,

$$20\,\mathrm{U}\,\mathrm{XX}\,\mathrm{YY}\,\mathrm{ab}\,12345 \tag{B.1}$$

The usage of the digits of the ATLAS18 wafers is listed in Table 8. The barrel short-strip (SS), long-strip (LS) sensors, and the endcap R0 to R5 sensors are identified with the letter in the digit "YY". The "Sensor generation-vendor", ATLAS18 and ATLAS17 with production, prototype, mechanical, etc. are identified with the letter in the digit "a". The sub-sensors or structures within a wafer are identified in the digit "b", such as Main sensor (0), QA pieces of Mini&MD8 (1), Testchip&MD8 (7), etc. The wafer number is identified with 5 digits under "12345".

Table 8: ATLAS Upgrade serial number scheme of the ATLAS18 wafers.

20 U XX YY ab 12345		
Digits	Usage	Letters
XX	Sub-detector Type	
	Strip Barrel	SB
	Strip Endcap	SE
	Strip General	SG
YY	Sensor Type	
	Long Strip, Barrel	SL
	Short Strip, Barrel	SS
	R0, Endcap	S0
	R1, Endcap	S1
	R2, Endcap	S2
	R3, Endcap	S3
	R4, Endcap	S4
	R5, Endcap	S5
a	Sensor Generation-Vendor	
	ATLAS18 production (HPK)	0
	ATLAS17 prototypes (HPK)	6
	(left open for future usage)	
	ATLAS18 prototypes (HPK)	8
	ATLAS18 mechanicals (HPK)	9
b	Sub-sensor Type	
	Main	0
	Mini&MD8 QA piece	1
	Mini SS (1x2.6 cm^2)	2
	Mini LS (1x5 cm^2)	3
	Diode (MD8)	4
	Wafer	5
	Miniature (1x1 cm^2) sensor	6
	Testchip&MD8 QA piece	7
	WBTS	8
	Halfmoon	9
1-5	Sensor numbering	
	Sequential number in 5 digits	12345

C Identification pad and scratch pads

The main sensors, halfmoons, and QA pieces have an identification label and scratch pads (the "ID"). The ID of the main sensor is shown in Fig. 15. The scratch pads have 6 blocks of 4 bits. The wafer number of 5 digits, 12345, can be scratched with binary-coded decimal numbers, using 5 blocks. The ID is placed near the bottom of the left edge of the main sensor, at the legend "Identification pads" in Fig. 2(a), e.g. The locations of the ID of the halfmoons, QA pieces, etc. in a wafer are indicated by the legends "...HM1", "...A1", etc., respectively, in Fig. 4 and 5.

Acknowledgments

We gratefully acknowledge Y. Abo, S. Kamada, K. Yamamura, and the team of engineers of HPK for their highly productive work on the designs, layouts, close communication and collaboration.

Fig. 15: Identification label and scratch pads.

This work was supported by the Canada Foundation for Innovation and the Natural Science and Engineering Research Council of Canada; the Ministry of Education, Youth and Sports of the Czech Republic coming from the projects LTT17018 Inter-Excellence and LM2018104 CERN-CZ and by Charles University grant GAUK 942119; the Spanish R&D grant PID2019-110189RB-C22, funded by MCIN/ AEI/10.13039/501100011033; the US Department of Energy, grant DE-SC0010107.

Copyright 2022 CERN for the benefit of the ATLAS Collaboration. CC-BY-4.0 license.

References

[1] *Technical Design Report for the ATLAS ITk Strip Detector*, CERN-LHCC-2017-005/ATLAS-TDR-025, April 1, 2017

[2] A. Ahmad et al., *The silicon microstrip sensors of the ATLAS semiconductor tracker*, Nuclear Inst. and Methods in Physics Research, **A 578** (2007) 98-118

[3] Y. Unno et al., *Development of n-on-p silicon sensors for very high radiation environments*, *Nucl. Instr. Meth.* **A 636** (2011) S24-S30

[4] Y. Unno et al., *Development of n^+-in-p large-area silicon microstrip sensors for very high radiation environments–ATLAS12 design and initial results*, Nuclear Inst. and Methods in Physics Research, **A 765** (2014) 80-90

[5] C. Lacasta et al., *Design of the first full size ATLAS ITk strip sensor for the endcap region*, Nuclear Inst. and Methods in Physics Research, **A 924** (2019) 137-141

[6] Y. Unno et al., *ATLAS17LS – A large-format prototype silicon strip sensor for long-strip barrel section of ATLAS ITk strip detector*, Nuclear Inst. and Methods in Physics Research, **A 989** (2021) 164928

[7] B. Hommels et al., *Detailed studies of full-size ATLAS12 sensors*, Nuclear Instruments and Methods in Physics Research, **A 831** (2016) 167-173

[8] K. Hara et al., *Charge collection study with the ATLAS ITk prototype silicon strip sensors ATLAS17LS*, Nuclear Inst. and Methods in Physics Research, **A 983** (2020) 164422

[9] M. Ullan et al, *Quality Assurance methodology for the ATLAS Inner Tracker strip sensor production*, Nuclear Inst. and Methods in Physics Research, **A 981** (2020) 164521

[10] A Chilingarov, *Temperature dependence of the current generated in Si bulk*, 2013 JINST 8 P10003

[11] M. Mikestikova et al, *ATLAS ITk strip sensor quality control procedures and testing site qualification*, 2022 JINST 17 C12013

[12] P. Allport et al, *Pre-production results from ATLAS ITk Strip Sensors Quality Assurance Testchip*, 2022 JINST 17 C11002, corresponding author: E. Bach

[13] I. Kopsalis et al, *Establishing the Quality Assurance Programme for the Strip Sensor Production of the ATLAS Tracker Upgrade Including Irradiation with Neutrons, Photons and Protons to HL-LHC Fluences*, preprint JINST_011P_1022, accepted for publication